Geophysical and Astrophysical Fluid Dynamics, 2013
Vol. 107, No. 4, 385–402, http://dx.doi.org/10.1080/03091929.2012.681782

New energy and helicity bounds for knotted and braided magnetic fields

RENZO L. RICCA*

Department of Mathematics and Applications, U. Milano-Bicocca,
Via Cozzi 53, 20125 Milano, Italy

(*Received 10 September 2011; in final form 29 February 2012; first published online 17 May 2012*)

In this article we present a review of some of the author's most recent results in topological magnetohydrodynamics (MHD), with an eye to possible applications to astrophysical flows and solar coronal structures. First, we briefly review basic work on magnetic helicity and linking numbers, and fundamental relations with magnetic energy and average crossing numbers of magnetic systems in ideal conditions. In the case of magnetic knots, we focus on the relation between their groundstate energy and topology, discussing the energy spectrum of tight knots in terms of *ropelength*. We compare this spectrum with the one given by considering the bending energy of such idealized knots, showing that curvature information provides a rather good indicator of magnetic energy contents. For loose knots far from equilibrium we show that inflexional states determine the transition to braid form. New lower bounds for tight knots and braids are then established. We conclude with results on energy-complexity relations for systems in presence of dissipation.

Keywords: Magnetic knots; Links; Braids; Energy spectrum; Ropelength; Helicity; Crossing number

1. Topological approach to the study of complex magnetic fields

Contrary to common perception, a topological study of magnetic fields has an already long history, rooted in the work of Gauss on geomagnetism (1832–1839) and in the remarkable observations of Maxwell, presented in his famous *Treatise on Electricity and Magnetism* (1873) in the wake of the then newborn vortex atom theory (for a mathematical reconstruction, see Ricca and Nipoti 2011). A revival took place with the realization of the topological interpretation of helicity (Moffatt 1969) and its applications in astrophysical contexts (Berger and Field 1984). In the last decades, topological dynamics received new impetus from work on physical knot theory, unified field theory, dynamical systems theory, as well as from direct numerical

*Email: renzo.ricca@unimib.it

simulations of complex systems. Much progress has been done in topological magnetohydrodynamics (MHD), in particular, as evidenced by recent publications (Arnold and Khesin 1998, Ricca 2001, 2009a,b): helicity has become an important indicator of magnetic structural complexity, that, in the case of the Sun (De Vore 2000, Démoulin and Berger 2003, Nindos *et al*. 2003) has been proven useful to measure morphological activity of coronal magnetic structures (Magara and Longcope 2003, Régnier *et al*. 2005); furthermore, energy-helicity relations and the role of energy minimizers in the topological relaxation of magnetic fields (Moffatt 1985) have led to a new search for energy groundstates of knots, links, and braids (Moffatt 1990, Berger 1993), that have involved other topologically related quantities, such as higher-order linking numbers, crossing numbers and ropelength information (see section 3 below); this research has stimulated further work on the role of these quantities in the re-structuring processes of coronal fields (Berger and Asgari-Targhi 2009, Wilmot-Smith *et al*. 2009) and in assessing energy budgets in the numerical diagnostics of the evolution of complex magnetic fields (Hauser *et al*. 2007, Del Sordo *et al*. 2010).

In this article we present an overview of some of the author's most recent results in topological MHD, with an eye to possible applications to astrophysical flows and solar coronal structures. Most of the results presented here are obtained in the context of ideal MHD, while the effects of change of topology in relation to strong dissipation are considered in the last section. By recalling standard definitions borrowed from knot theory and magnetic relaxation, we begin (section 2) with work on helicity and linking numbers of topologically complex systems, and then we consider fundamental relations with magnetic energy and average crossing numbers. In section 3, we consider zero-framed, tubular magnetic knots, seen as elementary components of complex physical systems, and we focus on the relation between groundstate energy and topology. Here, by introducing a new topological measure, the knot *ropelength*, we discuss the energy spectrum of tight knots in terms of ropelength by using data available from numerical simulations, and we compare this spectrum with the one given by considering the bending energy of such idealized knots. The two spectra have remarkable similarities, being indeed almost pointwise proportional to one another, suggesting that curvature information can be exploited to provide useful information on energy levels. For loose knots (far from equilibrium) inflexional states, occurring where there is a sudden change of concavity in the knot axis, influence the transition of these knots to form braids, with consequential energy re-distribution in the braid pattern: this issue is addressed in section 4, where indeed we show that inflexional knots do evolve to *spiral* (i.e. inflexion-free) knots and braids; a scenario consistent with the observed prevalence of braided solar coronal structures. New lower bounds for tight knots and braids are established in section 5. Finally (section 6), energy-complexity relations are examined for systems in the presence of strong dissipation.

2. Magnetic relaxation and topological bounds in ideal MHD

We consider magnetic knots and links in an ideal, incompressible, but perfectly conducting fluid in $\mathbb{R}^3$ (actually S^3). The magnetic field $\boldsymbol{B} = \boldsymbol{B}(\boldsymbol{x}, t)$ ($\boldsymbol{x}$ the position vector

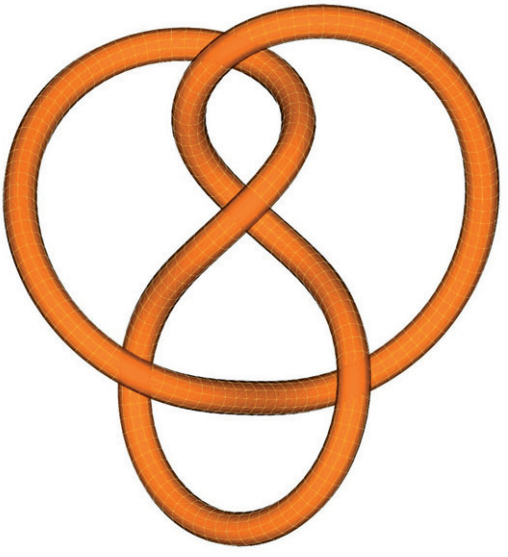

Figure 1. Magnetic knot given by embedding the magnetic field in a tube centred on the knot K_4^1.

and t time) is embedded in tubular loops, frozen in the fluid and with finite energy, that is

$$\boldsymbol{B} \in \{\nabla \cdot \boldsymbol{B} = 0,\ \partial_t \boldsymbol{B} = \nabla \times (\boldsymbol{u} \times \boldsymbol{B}),\ L_2\text{-norm}\}. \tag{1}$$

A magnetic knot K is given by embedding the magnetic field onto nested tori $\mathcal{T}_k$ $(k = 1, \ldots, m)$ in a cylindrical tube given by a *regular* tubular neighborhood $\mathcal{T}_a$, of radius $a > 0$, centred on the knot axis $\mathcal{C}$ of vector equation $\boldsymbol{X} = \boldsymbol{X}(s)$ (s arclength), local curvature $c = \|\mathrm{d}^2\boldsymbol{X}/\mathrm{d}s^2\|$ and radius of curvature $\rho = c^{-1}$ (see the example of figure 1). Regularity is ensured by taking $a \leq \rho$ pointwise along $\mathcal{C}$, and existence of non-self-intersecting nested tori in $\mathcal{T}_a$ is guaranteed by the tubular neighborhood theorem (Spivak 1979). $\mathcal{C}$ is assumed to be a C^3-smooth, closed loop (homeomorphic to the circle), simple (i.e. non-self-intersecting), and parametrized by arclength. The total length of $\mathcal{C}$ is $L = L(\mathcal{C})$. Evidently K has the knot type of $\mathcal{C}$, being either *trivial*, if $\mathcal{C}$ (the unknot) bounds a smoothly embedded disk, or *essential*. For simplicity, we take $\mathcal{T}_a = \mathcal{C} \otimes \mathcal{S}$ given by the product of $\mathcal{C}$ with the solid circular disk $\mathcal{S}$, uniform all along $\mathcal{C}$, of cross-sectional area $A = \pi a^2$. Hence, the total volume $V = V(\mathcal{T}_a) = \pi a^2 L$. We assume that the tubular boundary $\partial\mathcal{T}_a = \partial\mathcal{T}$ (dropping the suffix) be a magnetic surface at all times; by denoting with $\mathbf{v}_\perp$ the unit normal to $\partial\mathcal{T}$, we have

$$\mathrm{supp}(\boldsymbol{B}) := K \hookrightarrow \mathbb{R}^3, \quad \text{with} \quad \boldsymbol{B} \cdot \boldsymbol{v}_\perp = 0 \quad \text{on } \partial\mathcal{T}. \tag{2}$$

The magnetic flux Φ through the cross-section $\mathcal{S}$ is given by

$$\Phi = \int_{A(\mathcal{S})} \boldsymbol{B} \cdot \boldsymbol{v}\, \mathrm{d}^2\boldsymbol{x}, \tag{3}$$

where $\mathbf{v}$ is the unit normal to $\mathcal{S}$. $\{V, \Phi\}$ provides the *signature* of the magnetic knot K. The magnetic energy $M(t)$ and the magnetic helicity $H(t)$ are defined by:

$$M(t) = \frac{1}{2}\int_{V(K)} \|\boldsymbol{B}\|^2 \, \mathrm{d}^3\boldsymbol{x}, \tag{4}$$

and

$$H(t) = \int_{V(K)} \boldsymbol{A}\cdot\boldsymbol{B}\, \mathrm{d}^3\boldsymbol{x}, \tag{5}$$

where $\boldsymbol{A}$ is the vector (Coulomb) potential associated with $\boldsymbol{B} = \nabla\times\boldsymbol{A}$. As usual, we take $\nabla\cdot\boldsymbol{A} = 0$ in $\mathbb{R}^3$. Helicity is a conserved quantity of frozen fields (Woltjer 1958), thus in ideal MHD, we can set $H(t) = H = \text{constant}$.

When n magnetic knots are linked together, they form a magnetic link L_n, thus we can extend the definitions above also to links; hence, for example, we have

$$\mathrm{supp}(\boldsymbol{B}) := L_n \hookrightarrow \mathbb{R}^3, \quad \text{with} \quad \boldsymbol{B}\cdot\boldsymbol{v}_\perp = 0 \quad \text{on } \partial\mathcal{T}_i \quad \forall i = 1,\ldots,n, \tag{6}$$

with total volume $V = V(L_n)$.

It is well known that helicity admits topological interpretation in terms of linking numbers. Indeed we have (Moffatt 1969, Berger and Field 1984, Moffatt and Ricca 1992):

Theorem 2.1: *Let L_n be an essential magnetic link in an ideal fluid. Then, the magnetic helicity H of the link L_n is given by*

$$H = \sum_i Lk_i\,\Phi_i^2 + 2\sum_{i\neq j} Lk_{ij}\Phi_i\Phi_j, \tag{7}$$

where Lk_i denotes the Călugăreanu–White linking number of $\mathcal{C}_i$ with respect to the framing induced by the embedding of $\boldsymbol{B}$ in $\mathcal{T}_i$, and Lk_{ij} denotes the Gauss linking number of $\mathcal{C}_i$ with $\mathcal{C}_j$.

Lk_i and Lk_{ij} are two topological invariants of the link type. Lk_i measures the degree of internal linking of the $\boldsymbol{B}$-lines within each tubular component, that is, between the $\boldsymbol{B}$-lines of L_i and the knot axis $\mathcal{C}_i$, while Lk_{ij} measures the external linking between pairs of link components, that is between pairs of $\mathcal{C}_i$ and $\mathcal{C}_j$. *Zero-framing* denotes zero-linking ($Lk_i = 0$) of the magnetic field lines with $\mathcal{C}_i$, and this provides a gauge reference for helicity calculations.

Let us consider now the magnetic relaxation (Moffatt 1985) of a link L_n under a velocity field $\boldsymbol{u} = \boldsymbol{u}(\boldsymbol{x}, t)$, smooth function of the position vector $\boldsymbol{x}$, and time t (with $\nabla\cdot u = 0$ and $\boldsymbol{u} = 0$ at infinity). In ideal conditions, each link component is driven by the Lorentz force towards a minimum of magnetic energy. This evolution process is governed by a signature-preserving diffeomorphism associated with the magnetic transport equation (Faraday's law). The process is exemplified in figure 2 for the case of (a) a trefoil knot and (b) a Hopf link.

A fundamental problem in theory and applications is to establish rigorous relationships between energy and topological complexity of magnetic systems. Recent work in this direction can be summarized as follows. For simplicity, let us assume that

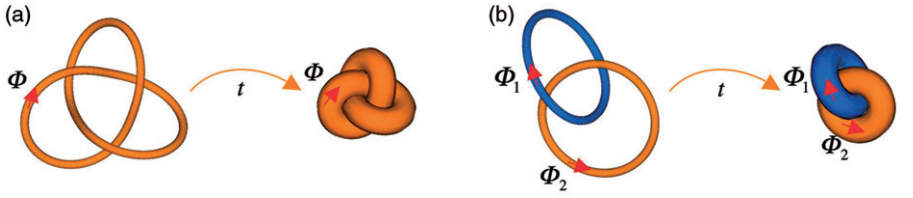

Figure 2. Magnetic relaxation of (a) a trefoil knot and (b) a Hopf link, under a volume- and flux-preserving flow.

all link components have equal flux $\Phi_i = \Phi$ and every knot is zero-framed. If $c_{\min}$ denotes the minimum crossing number (a topological invariant) of L_n, we have:

Theorem 2.2: *Let L_n be a zero-framed magnetic link in ideal conditions. Then*

$$\text{(i)} \quad M(t) \geq \left(\frac{2}{\pi V}\right)^{1/3} |H|; \quad \text{(ii)} \quad M_{\min} = \left(\frac{2}{\pi V}\right)^{1/3} \Phi^2 c_{\min}. \tag{8}$$

Proof of these results is based on works of Arnold (1974), Freedman and He (1991) and Ricca (2008).

2.1. *Discussion of results of Theorems 2.1 and 2.2*

Theorem 2.1 extends the original result of Moffatt (1969) to essential links, by establishing a fundamental relationship between the magnetic helicity of the link L_n, a conserved quantity of frozen fields evolution given by (5), and the topological character of the link in terms of linking numbers. From a practical viewpoint, (7) allows one to estimate the unknown quantities by using alternative methods. On one hand, helicity estimates can be directly obtained from either computations and numerical simulations based on (5), or from observational data. The calculation of the Gauss linking number Lk_{ij}, on the other hand, may be done by simply exploiting one of its equivalent interpretations given in terms of number of crossings (Ricca and Nipoti 2011). For this we make use of the concept of indented diagram of oriented curves. Given an n-component link, consider any pair of oriented components $\mathcal{C}_1$ and $\mathcal{C}_2$, and the projected diagram of these on a plane, by allowing indentations at each apparent crossing, for over- and under-crossings of the incident strands (figure 3). Since Lk_{ij} is a topological invariant of the link, its value does not depend on specific projections; therefore, *any* projection (obtained for instance by image analysis of observational data of real events) will provide the necessary and sufficient information for the calculation. Denoting by (Γ_i, Γ_j) a pair of incident strands of the link diagram, we have

$$Lk_{ij} = \frac{1}{2} \sum_{r \in \Gamma_i \sqcap \Gamma_j} \epsilon_r, \quad i \neq j, \tag{9}$$

where $\epsilon_r = \pm 1$ according to the algebraic sign convention associated with the apparent crossing at each intersection site $\Gamma_i \sqcap \Gamma_j$ (see the two examples of figure 3). Note that in

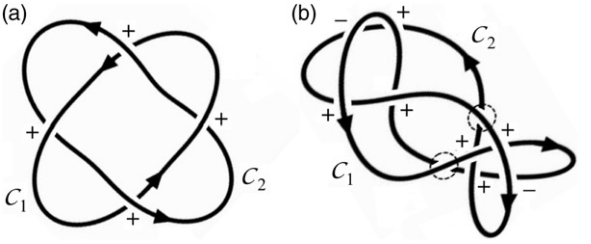

Figure 3. (a) Indented diagram resulting from the *minimal* projection of a two-component link with linking number $Lk_{12} = +2$; a + or − is assigned to each apparent crossing according to standard convention. (b) The same two-component link viewed from a different projection; the linking number calculation is independent of the projection plane. Note that the two self-crossing sites denoted by dashed circles do not contribute to the linking number computation.

the computation of the linking number we do not consider contributions from self-crossings. The total linking $Lk_{\rm tot}$ of an n-component link may then be defined as

$$Lk_{\rm tot} = \sum_{i,j} |Lk_{ij}|, \quad i \neq j. \tag{10}$$

For the calculation of the internal linking Lk_i we must recall the Călugăreanu–White formula

$$Lk_i = Wr_i + Tw_i, \tag{11}$$

where Wr_i and Tw_i denote, respectively, the writhing number and the total twist number of the i-th link component. Wr_i measures the average coiling and distortion of $\mathcal{C}_i$ in space, and depends on both curvature and torsion *of* $\mathcal{C}_i$. As for the actual calculation of the writhing number, we can resort to its interpretation in terms of signed crossings (Moffatt and Ricca 1992); thus, we have

$$Wr_i = \left\langle \sum_{r \in \Gamma_i \sqcap \Gamma_i} \epsilon_r \right\rangle, \tag{12}$$

where the angular brackets denote averaging over all (infinite) projections. In practice, a reasonable approximation of Wr_i is given by considering the diagrams obtained by taking any three mutually orthogonal projections of the same link, to get the estimated writhing number $Wr_{\perp_i}$ (Barenghi *et al.* 2001), that is

$$Wr_{\perp_i} = \left\langle \sum_{r \in (\Gamma_i \sqcap \Gamma_i)_{v_j}} \epsilon_r \right\rangle \quad (j = 1, 2, 3), \tag{13}$$

where v_j denotes a convenient projection direction.

Tw_i measures the average winding of the field-lines *around* $\mathcal{C}_i$, thus depending not only on the embedding of $\mathcal{C}_i$ in the ambient space, but also of the $\boldsymbol{B}$-lines within each $\mathcal{T}_i$. It is well-known (Moffatt and Ricca 1992), that the total twist Tw_i admits the decomposition $Tw_i = T_i + N_i$, given by the normalized total torsion T_i of $\mathcal{C}_i$ and the intrinsic twist N_i of the field lines around $\mathcal{C}_i$. The effect of the intrinsic twist of the field

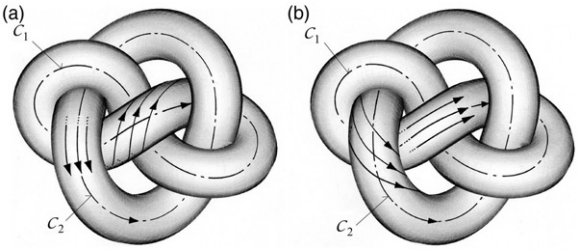

Figure 4. Examples of two-component magnetic link with five crossings, whose components are tubular unknots. Suppose both systems have $Lk_{12}=0$ and $\sum_{i=1,2}Lk_i=0$. By applying (11) to each link component, we have: (a) $Wr(\mathcal{C}_1)=+1$, $Tw(\mathcal{C}_1)=-1$, thus $Lk_1=0$ and $Wr(\mathcal{C}_2)=0$, $Tw(\mathcal{C}_2)=0$, thus $Lk_2=0$; (b) $Wr(\mathcal{C}_1)=+1$, $Tw(\mathcal{C}_1)=0$, thus $Lk_1=+1$ and $Wr(\mathcal{C}_2)=0$, $Tw(\mathcal{C}_2)=-1$, thus $Lk_2=-1$.

lines within each link component is shown in figure 4, where this is reflected in the total contribution to the linking of the magnetic system, and therefore to magnetic helicity.

In the case of solar loops, for instance, information on average intrinsic twist provides not only a measure of physical coherency and strength of the magnetic system, but also it gives some information on the amount of rotational energy inherited from photospheric motion. Since flux twist can only take values up to a critical threshold, above which a kink instability sets in (see section 4 below), twist helicity estimates are useful to get information on the torsional energy present. It should be noted, however, that Ricca and Maggioni (2007) showed that particularly simple kinematics based on a stretch-twist-fold model can produce unlimited amount of folding, while keeping an arbitrarily prescribed low bound on writhe and twist at all times, with consequential bound on total helicity (by (11)). (These types of kinematics, if supported by appropriate dynamics, would be particularly suitable for modeling fast dynamo actions.) Indeed, by combining (7) and (11), total helicity H can be decomposed into writhe and twist contributions, H_{Wr} and H_{Tw}. In particular, we have $H_{Tw}=H-H_{Wr}$. Hence, an estimate of H_{Tw} can be obtained by direct measurements of total helicity, using (5) and (13) by diagram extraction from visiometric analysis based on observational data and imaging analysis. These methods have been proven useful to study energy-complexity relationships in vortex tangles and turbulent flows (Barenghi *et al*. 2001) and will prove equally useful to examine astrophysical flows and complex morphologies of coronal fields.

Results of Theorem 2.2 establish lower bounds on the magnetic energy of zero-framed, essential links. Inequality (8)–(i) is the so-called ''realizability condition'', that states that the energy is bounded from below by the absolute value of the magnetic helicity divided by the average link size, given by $V^{1/3}$. Note that, as shown by the examples of figure 4, there are cases of essential links that in spite of their topological complexity, have linking number zero, hence helicity zero. For these cases inequality (8)–(i) is not so helpful, since it simply reduces to establish the positiveness of energy. Equation (8)–(ii), however, establishes an important, fundamental relationship between minimum magnetic energy and topology in terms of minimum number of crossings, that is $M_{\min}\propto c_{\min}$. This latter is a topological invariant, that can be estimated by minimizing the number of apparent crossings resulting from different projections of the same link, by applying, for example, a relaxation code to the link diagram. This technique can be implemented to give more accurate estimates for energy levels of force-

free fields in relation to possible eruptive events. In this sense, a search for these lower bounds may provide an alternative root to applications of Aly's theorem (Aly 1984) for potential magnetic field estimates. In any case, for a given $c_{\min}$ topology is not uniquely prescribed, therefore $c_{\min}$ must be interpreted as an average topological characterization of a given class of knots and links. For a one-to-one correspondence between energy and individual knot types, we need a more accurate approach, that takes into account the minimization of magnetic energy in knotted flux tubes. This approach will be examined in the following section.

3. Groundstate energy of zero-framed knots

Let us consider magnetic knots with the field confined to a single knotted flux tube K of signature (V, Φ) (V magnetic volume and Φ magnetic flux). Then, we have (Moffatt 1990):

Theorem 3.1: *The minimal magnetic energy $M_{\min}$ of K, attained under a signature-preserving flow, is given by*

$$M_{\min} = m(h)\Phi^2 V^{-1/3}, \tag{14}$$

where $m(h)$ is a positive dimensionless function of the dimensionless twist parameter h.

The fundamental problem posed by Moffatt (2001), that is to determine $m_{\min}$ (the value of $m(h)$ for which $M = M_{\min}$) for knots of minimum crossing number $c_{\min}$, is thus solved by applying Theorem 2.2–(ii) to (14). Hence, we have (Ricca 2008):

Corollary 3.2: *For zero-framed magnetic knots in ideal conditions we have*

$$m_{\min} = m(0) = (2/\pi)^{1/3} c_{\min}. \tag{15}$$

The functional dependence of M on h is of interest for applications. For this we consider a curvilinear, orthogonal coordinate system (r, ϑ_R, s), centred on the tube axis $\mathcal{C}$. The coordinates are given by the cross-sectional radius r, the azimuthal angle ϑ_R and the arc-length s along $\mathcal{C}$. Orthogonality is ensured by taking

$$\vartheta_R = \vartheta + \int_0^s \tau(\bar{s})\mathrm{d}\bar{s}, \tag{16}$$

where ϑ is a polar angle in the cross-sectional plane ($\vartheta = 0$ at some origin $s = 0$), and $\tau = \tau(s)$ is the torsion of $\mathcal{C}$. This system of coordinates provides a zero-twist reference frame on $\mathcal{C}$ in $\mathcal{T}$, and it can be used to calculate writhe and twist contributions. Now, let us assume that the magnetic field is given by

$$\boldsymbol{B} = \boldsymbol{B}_P + \boldsymbol{B}_T = B_{\vartheta_R}\hat{\boldsymbol{e}}_{\vartheta_R} + B_s\hat{\boldsymbol{t}}, \quad |\boldsymbol{B}_T| \gg |\boldsymbol{B}_P|, \tag{17}$$

where $\boldsymbol{B}_P$ and $\boldsymbol{B}_T$ denote poloidal and toroidal components along the azimuthal and axial directions given by the unit vectors $\hat{\boldsymbol{e}}_{\vartheta_R}$ and $\hat{\boldsymbol{t}}$ ($\hat{\boldsymbol{t}}$ unit tangent to $\mathcal{C}$). By using the solenoidal condition $\nabla \cdot \boldsymbol{B} = 0$, and after some algebra, we can express the magnetic

field in terms of poloidal and toroidal flux, Φ_P and Φ_T; we have (Maggioni & Ricca 2009)

$$\boldsymbol{B} = \left(0, \frac{1}{L}\frac{\mathrm{d}\Phi_P}{\mathrm{d}r}, \frac{1}{2\pi r}\frac{\mathrm{d}\Phi_T}{\mathrm{d}r}\right) + \left(0, \frac{\partial\widetilde{\psi}}{\partial s}, -\frac{\partial\widetilde{\psi}}{\partial\vartheta_R}\right), \tag{18}$$

where the total field is given by the sum of an average field plus a fluctuating field with zero net flux. The twist parameter (knot framing) is given by $h = \Phi_P/\Phi_T$. We shall use this result in the following.

3.1. *Knot framing and standard flux tube*

Let $V_r = \pi r^2 L$ be the partial volume of the tubular neighborhood of radius r; the ratio of the partial to total volume is given by $V_r/V(T) = (r/a)^2$. Now, let $f(r/a)$ be a monotonically increasing function of r/a; we can take

$$f(r/a) = \left(\frac{r}{a}\right)^{\gamma}, \quad (\gamma > 0). \tag{19}$$

Denoting by $\Phi \equiv \Phi_T(a)$ the total flux, we have

$$\Phi_T(r) = \left(\frac{r}{a}\right)^{\gamma}\Phi, \quad \Phi_P(r) = h\left(\frac{r}{a}\right)^{\gamma}\Phi, \tag{20}$$

where h, the twist parameter, denotes the *magnetic field framing*, given by $(2\pi)^{-1}$ times the turns of twist required to generate the poloidal field from the toroidal field, starting from $\Phi_P = 0$. A direct calculation of helicity in terms of fluxes (done in the Appendix A of Maggioni & Ricca 2009) shows that h is indeed the linking number Lk of the embedded field. The choice $\gamma = 2$ provides the prescription for a *standard* flux tube.

3.2. *Constrained relaxation to groundstate energy*

By applying standard variational methods the following result holds true (Maggioni & Ricca 2009):

Theorem 3.3: *Let K be an essential magnetic knot in an ideal fluid, of signature (V, Φ) and magnetic field given by* (18). *Moreover, let*

(i) *(V, Φ) be invariant;*
(ii) *the circular cross-section $\mathcal{S}$ be independent of arc-length s;*
(iii) *$\widetilde{\psi}$ be independent of arc-length s;*
(iv) *the knot length L be independent of h.*

Then, minimization of magnetic energy yields

$$M^* = \left(\frac{\gamma^2 L^{*2}}{8(\gamma-1)V} + \frac{\gamma\pi h^2}{2L^*}\right)\Phi^2, \tag{21}$$

where * denotes constrained minimum value.

Without loss of generality we can set $V=1$ and $\Phi=1$. Since the magnetic knot in the relaxed state is in tight configuration, we can introduce a non-dimensional parameter given by the aspect ratio of the tight knot, defined by the ratio of the minimal knot length L^* to the radius R^* of the maximal circular cross-section of the tight configuration; this ratio is the *ropelength* $\lambda = L^*/R^*$; of course $\lambda \geq 2\pi$, where $\lambda = 2\pi$ corresponds to the tight configuration of the torus (the unknot), when the hole collapses to a point. Thus, from $V = 1 = \pi R^{*2} \mathrm{L}^*$ we have

$$L^* = (\lambda^2/\pi)^{1/3}, \qquad R^* = (\pi\lambda)^{-1/3}. \tag{22}$$

Therefore, for standard flux tubes ($\gamma = 2$), equation (21) reduces to

$$M^*_\lambda(h) = \frac{\lambda^{4/3}}{2\pi^{2/3}} + \frac{\pi^{4/3}h^2}{\lambda^{2/3}}. \tag{23}$$

The absolute minimum is that given by the zero-framed unknot, by letting $h=0$ and $\lambda = \lambda_0 = 2\pi$; thus $M^*_\circ = (2\pi^2)^{1/3} \approx 2.70$. The groundstate energy of zero-framed flux tubes is a monotonic increasing function of ropelength (see figure 5, $h=0$); the minimum energy remains a monotonic increasing function of λ for framed flux tubes for $h \leq 2$: at $\lambda = \lambda_0 = 2\pi$, we have $M^*|_{h=1} = 4.05$ and $M^*|_{h=2} = 8.11$. For $h \geq 2$ the energy minimum is attained at $\lambda = h\pi$, and for $h > 2$ the functional dependence of M^* on λ is no longer monotonic.

By using ropelength data from knot tightening simulations obtained by SONO relaxation algorithm (Pieranski 1998, Baranska *et al.* 2005) and, from (23), by letting $M^*_\lambda(0) = \lambda^{4/3}/2\pi^{2/3}$, we obtain the groundstate energy spectrum of the first 250 prime knots. Let us normalize the energy levels with respect to the minimum energy value $M^*_\circ$ of the tight torus; we have

$$\tilde{M} = \frac{M^*_\lambda(0)}{M^*_\circ} = \left(\frac{\lambda}{2\pi}\right)^{4/3} = \left(\frac{\lambda}{\lambda_0}\right)^{4/3}. \tag{24}$$

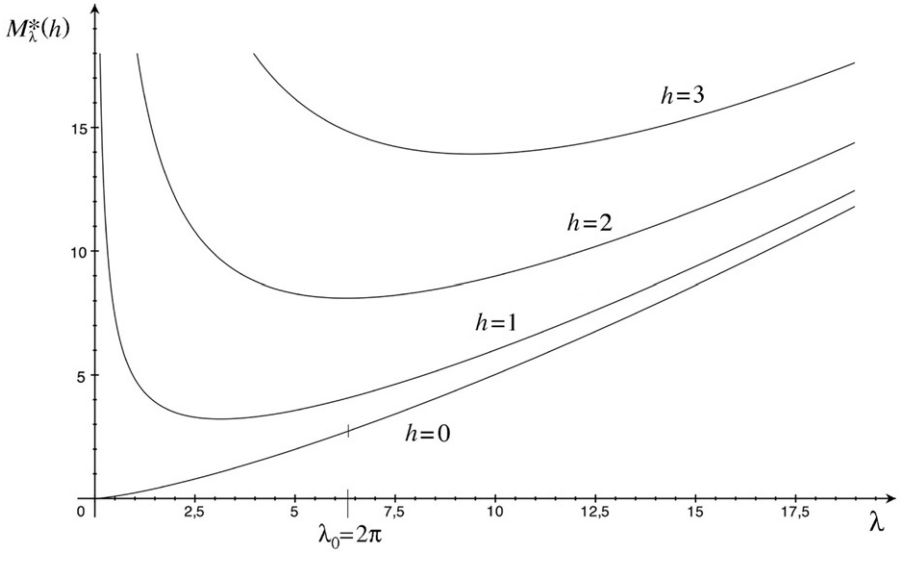

Figure 5. Constrained groundstate energy plotted against ropelength for different values of framing.

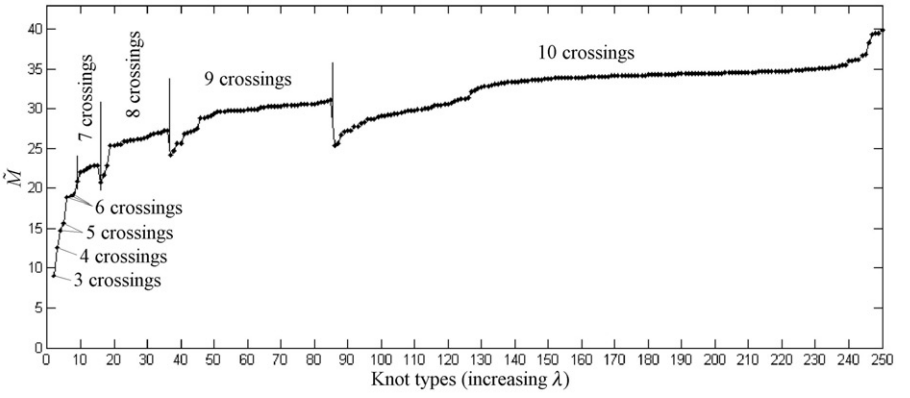

Figure 6. Groundstate energy spectrum of $\tilde{M}$ for the first 250 prime knots ($h=0$), plotted against increasing ropelength λ within each family of $c_{\min}$.

The energy spectrum of $\tilde{M}$ for the first 250 prime knots, plotted for increasing ropelength within each family of minimum number of crossing, is shown in figure 6. Drops in energy levels correspond to the presence of non-alternating sequence of positive and negative crossings in the knot (minimal) diagram (non-alternating knots); according to (8)–(ii), though, the average value of the energy levels within each knot family (i.e. for given $c_{\min}$) increases with crossing number.

It is interesting to compare this spectrum with another energy spectrum, obtained by considering the bending energy in place of the magnetic energy. Since magnetic relaxation is driven by the Lorentz force, that is mainly a curvature force (see section 4 below), computation of the energy due to curvature (bending energy) of tight knots provides an interesting comparison. Bending energy is defined by

$$E_b = \frac{1}{2}\oint_{\mathcal{C}} K_b[c(s)]^2 \,\mathrm{d}s, \tag{25}$$

where K_b is bending rigidity and $c(s)$ is local curvature. By normalizing this quantity with respect to the reference value $E_\circ = \pi K_b/R^* = K_b 2^{1/3}\pi^{5/3}$ of the tight torus (where we have made use of the second of (22)), we have the normalized bending energy

$$\tilde{E} = \frac{E_b}{E_\circ} = \frac{\oint_{\mathcal{C}}[c(s)]^2 \,\mathrm{d}s}{2^{4/3}\pi^{5/3}}. \tag{26}$$

By using curvature data of tight knots obtained by SONO, we can easily compute the energy spectrum $\tilde{E}$ of the first 250 prime knots for increasing ropelength. Data are shown in figure 7; direct comparison of the spectra of magnetic and bending energy shows that $\tilde{M}/\tilde{E}$ is almost pointwise constant for sufficiently large $c_{\min}$, indicating a good correspondence between magnetic energy minima and curvature information.

4. From inflexional knots to inflexion-free braids

During evolution magnetic fields tend to develop twists. Indeed twisted configurations occur naturally in the ambient fluid and are ubiquitous in the Solar corona. Solar loops

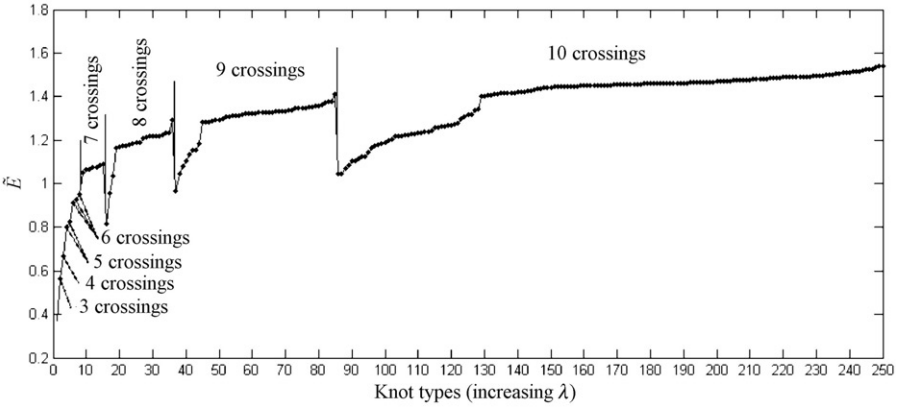

Figure 7. Spectrum of the normalized bending energy $\tilde{E}$, plotted against increasing ropelength λ within each family of $c_{\min}$.

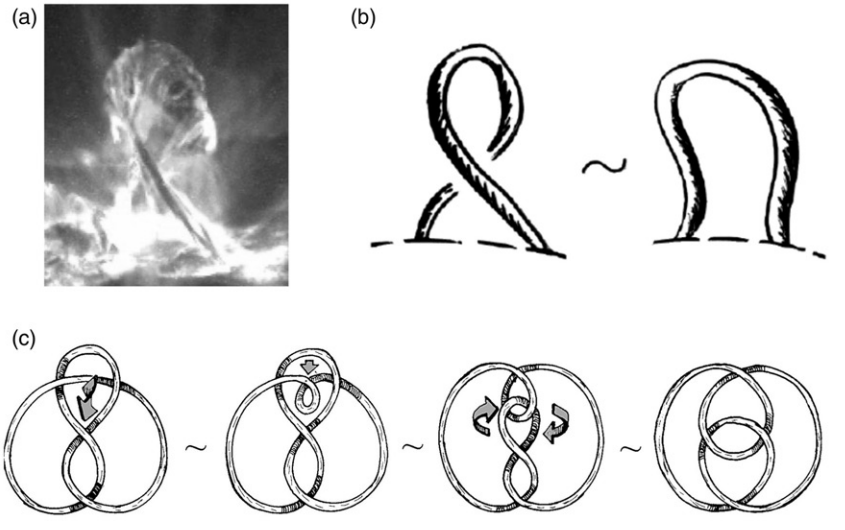

Figure 8. (a) *TRACE* satellite observation of filament destabilization in the Solar photosphere (Active Region 9957) on May 27, 2002. (b) A twist move (a Reidemeister type I move) on a tube strand. (c) By a sequence of consecutive twist moves a figure-of-eight knot (far left) is deformed to a closed braid (far right).

develop twists (figure 8(a)) as they rise from the photosphere (Fan and Gong 2000) and, as a consequence of continuous accumulation of torsional energy, may become unstable; twisting of field lines builds up and eventually saturates at about two full turns of twist, when the flux-tube reaches a critical threshold for kink instability, just before flaring up in the corona (Ricca 1997, Titov and Démoulin 1999). A simple calculation shows that in the incompressible limit the kink instability threshold of magnetic flux

tube and the writhing instability of elastic rods, where loops develop from the excess twist, occur almost at the same value: a further evidence of the "elastic" response of magnetic field to curvature forces.

Under conservation of helicity (see (11)), a twist move on a tube strand (called *Reidemeister type I move*, figure 8(b)) performs an exchange of twist and writhe helicity, a fundamental process for energy re-distribution in active regions (López Fuentes *et al*. 2003). As shown by Moffatt and Ricca (1992), writhe and twist exchange is invariably associated with a generic passage through an inflexion point, that is a point of zero curvature in isolation. Inflexional configurations are states defined by the presence of an inflexion point associated with a change of concavity, as in an S-shaped plane curve. By using the coordinate system introduced in section 3, we can compute the Lorentz force associated with the magnetic field (18); in particular we have (Ricca 1997)

$$\boldsymbol{F}_{\perp} = {B_s}^2 \frac{c}{K}\hat{\boldsymbol{n}} - \left[\frac{{B_\theta}^2}{r} + \frac{1}{2}\frac{\partial}{\partial r}\left({B_\theta}^2 + {B_s}^2\right)\right]\hat{\boldsymbol{e}}_r, \tag{27}$$

where $\boldsymbol{F}_{\perp}$ denotes the perpendicular component of the force to the tube axis, $K = 1 - cr\cos\vartheta$ is a scale factor, and $\hat{\boldsymbol{n}}$ and $\hat{\boldsymbol{e}}_r$ are unit normal and radial vector, respectively. This force induces a displacement of the magnetic field lines along the principal normal direction. Since inflexional states are loci of local change of curvature, the perpendicular component of the Lorentz force flips direction through an inflexion point. Indeed direct calculation of the Lorentz force for a generic passage through an inflexional state yields a deformation instability. We have (Ricca 2005):

Theorem 4.1: *Let K be an essential magnetic knot in an ideal fluid, of signature (V, Φ) and magnetic field given by* (18). *Let $\tilde{K}_t$ denote the generic, time-dependent passage of K through an inflexional state at time $t = t_0$. Then, the magnetic knot $\tilde{K}_{t_0}$ is in inflexional disequilibrium.*

Therefore, inflexional flux tubes re-arrange themselves to inflexion-free configurations: inflexional magnetic knots evolve to *spiral* knots (i.e. knots free from inflexions), according to the following (Ricca 2005):

Corollary 4.2: *A loose inflexional magnetic knot $\tilde{\mathcal{K}}_{t_0}$ evolves to a spiral knot $\mathcal{K}_t$ for any $t > t_0$.*

Spiral knots are indeed inflexion-free braids. As conjectured by Ricca (1997), inflexion-free braids result from the natural re-arrangement of inflexional magnetic fields in disequilibrium (see figure 9). From a topological viewpoint it is well-known that every knot can be isotoped to a closed braid by a sequence of twist moves, as shown in the example of figure 8(c). Magnetic braids under curvature forces deform then to inflexion-free configurations. Work on relationships between geometric and topological properties of closed braids with or without inflexions is currently under way (Colin Adams, private communication).

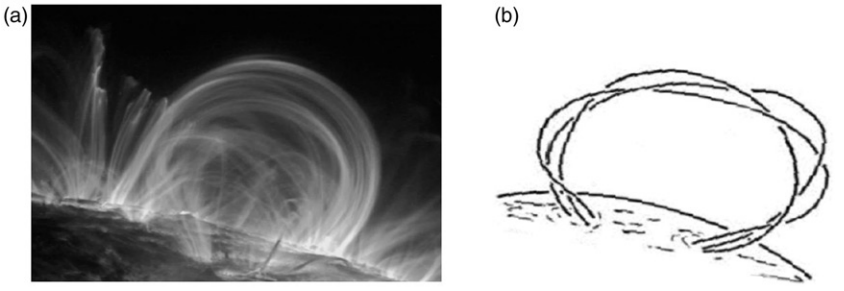

Figure 9. (a) *TRACE* satellite observation of solar loops in an active region. (b) Diagrammatic representation of braided magnetic fields in solar loops.

5. New lower bounds for tight knots and braids

We can establish a new lower bound for tight knots by combining (8)–(ii) and (23), by setting $h=0$ (zero framing) and $V=\Phi=1$; we have

$$M^*_\lambda(0)=\frac{\lambda^{4/3}}{2\pi^{2/3}}\geq M_{\min}=\left(\frac{2}{\pi}\right)^{1/3}c_{\min}. \tag{28}$$

This gives

$$\lambda=\frac{L^*}{R^*}\geq(16\pi)^{1/4}c_{\min}^{3/4}\approx 2.66\,c_{\min}^{3/4}. \tag{29}$$

Inequality (29) provides one of the best analytical bounds for tight knots of *any* $c_{\min}$. However, numerical simulations show (Baranska *et al*. 2004) that this bound is far from strict. Analytical tighter bounds could be achieved by relaxing some of the constraints imposed on the process, the first and most constraining being the circularity of the cross-section. Indeed, as the tube strands come into contact during relaxation, a more accurate modeling of the ''close approach'' state would certainly provide a much better estimate of the equilibrium stage. The analytical problem involves a three-dimensional study of the shape of the tube boundary near equilibrium, that is certainly not a trivial task. Results on rod packing with elliptical cross-sections (Lidin *et al*. 1995), for instance, could provide some help to estimate the free volume arising from interstices.

We can use the results above to establish also a lower bound for generic braids. By using the inequality (Ohyama 1993)

$$c_{\min}\geq 2(b-1), \tag{30}$$

where b is the *braid index*, given by the minimum number of strings in the braid representation of the knot, and (29), we have

$$M_{\min}\geq\left(\frac{16}{\pi}\right)^{1/3}(b-1),\quad\text{and}\quad\lambda\geq 4\left(\frac{\pi}{2}\right)^{1/4}(b-1)^{3/4}. \tag{31}$$

Since for a given braid the braid index is a topological quantity, the first inequality of (31) provides another interpretation of minimum energy in terms of topology.

6. Energy-complexity relations for dissipative systems

In presence of strong, dissipative effects the topology of magnetic fields is bound to change due to reconnections, hence $H = H(t)$. The rate of change of magnetic helicity can be related to the change in crossing number. A useful algebraic measure of complexity is given by the average crossing number $\overline{C}$, that counts the overall number of apparent crossings present in an entangled system of filaments. This quantity is defined as the sum of all unsigned crossings present in the system, averaged over-all projections. For any pair of closed curves $\mathcal{C}_i$, $\mathcal{C}_j$, we have

$$\overline{C}_{ij} = \left\langle \sum_{r \in \mathcal{C}_i \# \mathcal{C}_j} |\epsilon_r| \right\rangle, \tag{32}$$

where # denotes the total number of apparent intersections, including self-crossings, averaged over all directions of projection. For two links almost planar, such as those of figure 3, we have (a) $\overline{C}_{12} = 4$ and (b) $\overline{C}_{12} = 10$. This measure can be easily extended to any number of curves and, in general, $\overline{C} = \overline{C}(t)$. The following result holds true (Ricca 2008):

Theorem 6.1: *Let L_n be a zero-framed, essential magnetic link, embedded in a resistive, incompressible fluid. Then, we have*:

$$\text{(i)} \quad |H(t)| \leq 2\Phi^2 \overline{C}(t); \quad \text{(ii)} \quad \left| \frac{\mathrm{d}|H(t)|}{\mathrm{d}t} \right| \leq 2\Phi^2 \left| \frac{\mathrm{d}\overline{C}(t)}{\mathrm{d}t} \right|. \tag{33}$$

The average crossing number is a quantity that can be easily estimated by approximating $\overline{C}$ with $\overline{C}_\perp$, obtained by extracting average crossing number information from three mutually orthogonal planes of projections, as was done for the estimated writhing number of (13).

For solar coronal fields estimates on helicity dissipation made by Berger (1984) show that for typical coronal loops $\mathrm{d}H/\mathrm{d}t$ scales at most as $\mathrm{Re}_\mathrm{m}^{-1/2}$ (where Re_m is the magnetic Reynolds number), but it can be even smaller at high Re_m, so that inequality (33)–(ii) has real meaning only when a net change in the number of crossings is massive. Dissipation of energy, though, may be considerable even at high Reynolds numbers. In presence of random photospheric motion Berger (1993) found that the free energy of an N-component magnetic braid is given by

$$E_f \propto \frac{c_{\min}^2 \Phi^2}{N^2 L}, \quad \text{with} \quad c_{\min} \propto N^{3/2}, \tag{34}$$

so that

$$E_f \propto \frac{\Phi^2}{L} N. \tag{35}$$

By using Ohyama inequality and the first of (31) above, we have

$$M_{\min} \propto \frac{\Phi^2}{L}(N-1), \tag{36}$$

that is not only in good agreement with (35) above, but it clearly indicates that the linear relation between energy and number of braid components remains valid even at a fundamental energy level. Interesting work relating braiding complexity level and energy in coronal loops has been carried out by Berger and Asgari-Targhi (2009) and, more recently, by Hornig and collaborators (Pontin *et al*. 2011, Wilmot-Smith *et al*. 2011).

7. Concluding remarks

In this article we have reviewed some of the author's most recent results on topological MHD, with an eye to possible applications to astrophysical flows and solar coronal structures. Basic work on the interpretation of magnetic helicity in terms of linking numbers has been reviewed, highlighting its computation by means of crossing number information. These methods have been used in test cases using data obtained by numerical simulations and they will be useful in the numerical diagnostics of large data sets obtained from observations or numerical simulations. Two fundamental inequalities between magnetic energy and structural complexity have been presented and discussed. The first is the so-called ''realizability condition'', that provides a lower bound for the magnetic energy of a given link in terms of helicity and average size of the link system. The second inequality prescribes a lower bound for the minimum magnetic energy in terms of minimum number of crossings, thus establishing a fundamental relation between topological complexity and lowest energy levels. Nevertheless, complex systems of different topology may still have same topological crossing number: the standard knot table, for instance, provides many examples of different knot types with same minimum number of crossings. Hence, a one-to-one correspondence between (zero-framed) knot types and energy minima is required; this is done in section 3 by the equation (21) of Theorem 3.3. By normalizing everything with respect to the tight unknot energy, we obtain (24), that allows us to determine the energy spectrum of the first 250 prime knots in terms of their ropelength, a good indicator of knot complexity. This spectrum shows how the constrained minimum energy grows pointwise (and on average) with knot complexity. Direct comparison with the spectrum obtained by the normalized bending energy of tight knots reveals that at increasing crossing number the two energy spectra are almost pointwise proportional to one another, suggesting that curvature information is indeed a good indicator of the energy content of magnetic systems.

Inflexional configurations, characterized by a sudden change of concavity in the magnetic field line, are ubiquitous in magnetic structures. For loose knots these are states of instability and disequilibrium (Theorem 4.1). Inflexional magnetic fields remove their inflexion points by re-arranging their shape to inflexion-free knots (spiral knots) and braids. This result provides theoretical grounds to the observation of abundant braided patterns in the solar corona (see figure 9).

New lower bounds for the ropelength of tight knots and braids in terms of minimum crossing number and braid index are established in section 5. Finally, in section 6, we consider energy-complexity relations for magnetic systems in the presence of dissipation. The change in helicity is determined in terms of change in average crossing number and, by using Oyhama inequality, we show that for braided patterns the minimum

energy levels are proportional to the braid index given by the minimum number of components of the braid type, a result that confirms and extends Berger's (1984) result to minimum energy configurations.

With this review, we hope to have given sufficient information to the interested reader about the relevance and usefulness of topological methods and results in magnetic field theory and astrophysics. With the ever growing computational power and data acquisition capability, we believe that several ideas and methods based on concepts outlined here will be profitably employed to explore energy-complexity relations and to tackle outstanding questions concerning energy and helicity distribution in complex magnetic systems.

Acknowledgments

R.L.R. wishes to thank Francesca Maggioni for her help to produce the plots of figures 6 and 7 based on SONO data.

References

Aly, J.J., On some properties of force-free magnetic fields in infinite regions of space. *Astrophys. J.* 1984, **283**, 349–362.

Arnold, V.I., The asymptotic Hopf invariant and its applications; in *Proceedings of the Summer School in Differential Equations at Dilizhan*, 1974, pp. 229–256 (Erevan: Armenian Acad. Sci.). [English translation: *Sel. Math. Sov.* 1986 **5**, 327–345].

Arnold, V.I. and Khesin, B.A., *Topological Methods in Hydrodynamics*. Applied Mathematical Sciences, Vol. 125, 1998. (Berlin: Springer-Verlag).

Baranska, J., Pieranski, P., Przybyl, S. and Rawdon, E.J., Length of the tightest trefoil knot. *Phys. Rev. E* 2004, **70**, 051810–1-051810-9.

Baranska, J., Pieranski, P. and Rawdon, E.J., Ropelength of tight polygonal knots. In *Physical and Numerical Models in Knot Theory*, edited by J.A. Calvo, *et al*., pp. 293–321, 2005, Series on Knots and Everything, Vol. 36 (World Scientific: Singapore).

Barenghi, C.F., Ricca, R.L. and Samuels, D.C., How tangled is a tangle?. *Physica D* 2001, **157**, 197–206.

Berger, M.A., Rigorous new limits on magnetic helicity dissipation in the solar corona. *Geophys. Astrophys. Fluid Dyn.* 1984, **30**, 79–104.

Berger, M.A., Energy–crossing number relations for braided magnetic fields. *Phys. Rev. Lett.* 1993, **70**, 705–708.

Berger, M.A. and Asgari-Targhi, M., Self-organized braiding and the structure of coronal loops. *Astrophys. J.* 2009, **705**, 347–355.

Berger, M.A. and Field, G.B., The topological properties of magnetic helicity. *J. Fluid Mech.* 1984, **147**, 133–148.

De Vore, C.R., Magnetic helicity generation by solar differential rotation. *Astrophys. J.* 2000, **539**, 944–953.

Del Sordo, F., Candelaresi, S. and Brandenburg, A., Magnetic-field decay of three interlocked flux rings with zero linking number. *Phys. Rev. E* 2010, **81**, 036401–036407.

Démoulin, P. and Berger, M.A., Magnetic energy and helicity fluxes at the photospheric level. *Sol. Phys.* 2003, **215**, 203–215.

Fan, Y. and Gong, D., On the twist of emerging flux loops in the solar convection zone. *Sol. Phys.* 2000, **192**, 141–157.

Freedman, M.H. and He, Z.-X., Divergence-free fields: energy and asymptotic crossing number. *Ann. Math.* 1991, **134**, 189–229.

Hauser, H., Hagen, H. and Theisel, H. (editors), *Topology-based Methods in Visualization*, 2007 (Berlin: Springer-Verlag).

Lidin, S., Jacob, M. and Andersson, S., A mathematical analysis of rod packings. *J. Solid State Chem.* 1995, **114**, 36–41.

López Fuentes, M.C., Démoulin, P., Mandrini, C.H., Pevtsov, A.A. and van Driel-Gesztelyi, L., Magnetic twist and writhe of active regions. *Astron. & Astrophys*. 2003, **397**, 305–318.
Magara, T. and Longcope, D.W., Injection of magnetic energy and magnetic helicity into the solar atmosphere by an emerging magnetic flux tube. *Astrophys. J*. 2003, **586**, 630–649.
Maggioni, F. and Ricca, R.L., On the groundstate energy of tight knots. *Proc. R. Soc. A* 2009, **465**, 2761–2783.
Moffatt, H.K., The degree of knottedness of tangled vortex lines. *J. Fluid Mech*. 1969, **35**, 117–129.
Moffatt, H.K., Magnetostatic equilibria and analogous Euler flows of arbitrarily complex topology. Part I. Fundamentals. *J. Fluid Mech*. 1985, **159**, 359–378.
Moffatt, H.K., The energy spectrum of knots and links. *Nature* 1990, **347**, 367–369.
Moffatt, H.K., Some remarks on topological fluid mechanics. In *An Introduction to the Geometry and Topology of Fluid Flows*, edited by R.L. Ricca, pp. 3–10, 2001, NATO Science Series, II Mathematics, Physics and Chemistry, Vol. 47 (Kluwer Acad. Publs.: Dordrecht).
Moffatt, H.K. and Ricca, R.L., Helicity and the Călugăreanu invariant. *Proc. R. Soc. Lond. A* 1992, **439**, 411–429.
Nindos, A., Zhang, J. and Zhang, H., The magnetic helicity budget of solar active regions and coronal mass ejections. *Astrophys. J*. 2003, **594**, 1033–1048.
Ohyama, Y., On the minimal crossing number and the braid index of links. *Canad. J. Math*. 1993, **45**, 117–131.
Pieranski, P., In search of ideal knots. In *Ideal Knots*, edited by A. Stasiak, *et al*., pp. 20–41, 1998, Series on Knots and Everything, Vol. 19 (World Scientific: Singapore).
Pontin, D.I., Wilmot-Smith, A.L., Hornig, G. and Galsgaard, K., Dynamics of braided coronal loops II. Cascade to multiple small-scale reconnection events. *Astron. & Astrophys*. 2011, **525**, A57.
Régnier, S., Amari, T. and Canfield, R.C., Self and mutual helicities in coronal magnetic configurations. *Astron. & Astrophys*. 2005, **442**, 345–349.
Ricca, R.L., Evolution and inflexional instability of twisted magnetic flux tubes. *Sol. Phys*. 1997, **172**, 241–248.
Ricca, R.L. (editor), *An Introduction to the Geometry and Topology of Fluid Flows*, NATO ASI Series II, Vol. 47, 2001. (Kluwer: Dordrecht).
Ricca, R.L., Inflexional disequilibrium of magnetic flux tubes. *Fluid Dyn. Res*. 2005, **36**, 319–332.
Ricca, R.L. and Maggioni, F., A new stretch-twist-fold model for fast dynamo. *Proc. Appl. Math. Mech*. 2007, **7**, 2100051–2100052.
Ricca, R.L., Topology bounds energy of knots and links. *Proc. R. Soc. A* 2008, **464**, 293–300.
Ricca, R.L., New developments in topological fluid mechanics. *Nuovo Cimento C* 2009a, **32**, 185–192.
Ricca, R.L. (editor), *Lectures on Topological Fluid Mechanics*, Springer-CIME Lecture Notes in Mathematics, Vol. 1973, 2009b. (Springer-Verlag: Heidelberg).
Ricca, R.L. and Nipoti, B., Gauss' linking number revisited. *J. Knot Theory & Its Ram*. 2011, **20**, 1325–1343.
Spivak, M., *A Comprehensive Introduction to Differential Geometry*, Vol. 1, 1979. (Houston: Publish or Perish).
Titov, V.S. and Démoulin, P., Basic topology of twisted magnetic configurations in solar flares. *Astron. & Astrophys*. 1999, **351**, 707–720.
Wilmot-Smith, A.L., Hornig, G. and Pontin, D.I., Magnetic braiding and parallel electric fields. *Astrophys. J*. 2009, **696**, 1339–1347.
Wilmot-Smith, A.L., Pontin, D.I., Yeates, A.R. and Hornig, G., Heating of braided coronal loops. *Astron. & Astrophys*. 2011, **536**, A67.
Woltjer, L., A theorem on force-free magnetic fields. *Proc. Natl. Acad. Sci. USA* 1958, **44**, 489–491.